Research Article

Deployment/Retrieval Modeling of Cable-Driven Parallel Robot

Q. J. Duan,[1] J. L. Du,[1] B. Y. Duan,[1] and A. F. Tang[2]

[1] *School of Mechano-Electronic Engineering, Xidian University, Xi'an, Shaanxi 710071, China*
[2] *School of Mechano-Electronic Engineering, Xi'an University of Technology, Xi'an, Shaanxi 710048, China*

Correspondence should be addressed to Q. J. Duan, qjduan@126.com

A steady-state dynamic model of a cable in air is put forward by using some tensor relations. For the dynamic motion of a long-span Cable-Driven Parallel Robot (CDPR) system, a driven cable deployment and retrieval mathematical model of CDPR is developed by employing lumped mass method. The effects of cable mass are taken into account. The boundary condition of cable and initial values of equations is founded. The partial differential governing equation of each cable is thus transformed into a set of ordinary differential equations, which can be solved by adaptive Runge-Kutta algorithm. Simulation examples verify the effectiveness of the driven cable deployment and retrieval mathematical model of CDPR.

1. Introduction

Cable systems arise in many practical applications, such as bridges, underwater systems, aircraft decoy systems, and tethered satellite systems. When cables are utilized to replace links to the feed cabin to track radio source in 500 m aperture spherical radio telescope, we get Cable-Driven parallel robot (CDPR), which is developed from parallel and serial cable-driven robot. Conventional robots with serial or parallel structures are impractical for some applications since the workspace requirements are higher than what the conventional robots can provide. CDPR which uses cables instead of links to manipulate objects reduces the structural weight considerably in [1, 2]. The cables are so light that actuators of CDPR have only to drive their loads. Furthermore, CDPR gives a wide range of motion, because drums of the mechanism can wind long cables. For the above reasons, cable-driven mechanisms have received attention and have been recently studied since the 1980s [3]. Some reported researches on CDPR are NIST Robocrane [4], ultrahigh speed robot, tendon-driven Stewart
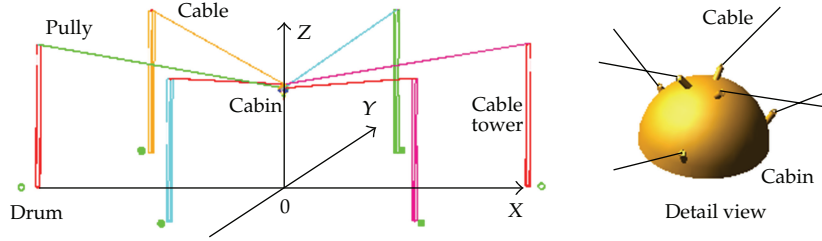
Figure 1: The 50 m scaled model.

platform, parallel wire mechanism for measuring a robot pose, controller designs for CDPR [5], and wrench-feasible workspace analysis for CDPR [6].

Particularly, dynamical characteristics of this type of mechanism have been well studied, such as the manipulation problem of load by multiple wires [7, 8], and the cables are considered to be massless. However, the cable will extend when stretched, and an error in length of 0.1% can give rise to an error in force of about 50%, thus accurate modeling of the cables is crucial [9].

Methods for approximating the cable motion and its equilibria have been studied for many years. Cable-body systems have been modeled using continuum models based on partial differential equations for strings, as well as lumped mass method in [10]. In complex applications, the lumped mass method representation is usually the preferred choice for detailed simulation work [11] and is employed in our work.

In this paper, we present a deployment and retrieval cable mathematical model using a lumped parameter representation. First, the general representation of the cable model is given. Then, according to the 50 m scaled model (Figure 1), based on the inverse kinematics analysis, the inverse dynamic formulation of deployment and retrieval CDPR is established. Finally, numerical simulations illustrate the performance of the proposed method.

2. Mathematical Model for Cable

A simple schematic of the CDPR for 50 m scaled model representing the coordinate systems is shown in Figure 1, and cable coordinate system is showed in Figure 2. The CDPR is considered that is kinematically and statically determined. In the design, there is a cable tower/winch pair at each vertex of a regular hexagon of radius α, which actuates six cables that are linked to a cabin. Therefore, the cabin can translate and rotate in the inertial frame. Let the origin of the inertial frame OXYZ be the center of the six towers [12].

In this model, the cable is assumed to be idea extensible and uniform in mass and the torsional deformation is ignored. The cable is approximated through the linear stress-strain relationship. The section is circle, and the cable is deployed from one end mass only. A representation of the model, as well as the generalized coordinates used to describe the motion, is shown in Figure 2. Let ($\tau, \mathbf{n},$ and $\mathbf{b}$) represent the unit vectors of the cable frame. The rotation matrix ^oR transforms S from the cable frame to the inertial frame OXYZ. s represents the length coordinate of the unstretched cable measured form its downstream end. When the cable is stressed, the length is $S(s,t)$. Cable satisfies the following relation: $dS = (\partial S/\partial s)ds$. According to the mechanics of elasticity relationship between Strain ε and Stress $\mathbf{T}$, we get: $\varepsilon = T/EA_0$ and $\varepsilon = (dS - ds)/ds \Rightarrow \partial S/\partial s = 1 + \varepsilon$.
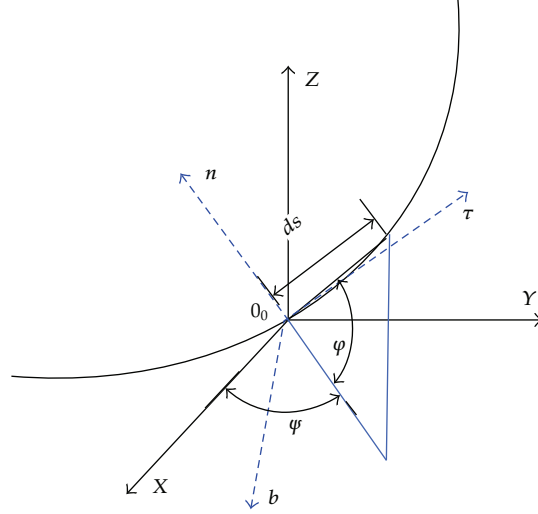
Figure 2: Fixed and cable coordinate system.

In the above equation, $\mathbf{r}(s,t)$ is the position vector of a point on the continuous cable, E is Young's modulus, and A_0 is the unstressed cross-sectional area. Considering a cable element located at point P at time t, Its inertial position is given by the vector $\mathbf{r}(s,t) : [t_0, \infty) \times [0, L] \rightarrow R^3$, which satisfies the relation $\mathbf{r}(s,t) = [x(s,t), y(s,t), z(s,t)]^T$.

$$\tau = \frac{\partial \mathbf{r}}{\partial S}, \tag{2.1}$$

$$\boldsymbol{\tau}(s,t) = \frac{\partial s}{\partial S}\frac{\partial \mathbf{r}}{\partial s} = \frac{1}{1+\varepsilon}\frac{\partial \mathbf{r}}{\partial s} = \frac{1}{1+\varepsilon}\left(\frac{\partial x}{\partial s}\mathbf{i} + y\frac{\partial y}{\partial s}\mathbf{j} + \frac{\partial z}{\partial s}\mathbf{k}\right). \tag{2.2}$$

The axial strain along the curve is approximated by

$$\varepsilon = \frac{1}{2}\left(\frac{\partial \mathbf{r}}{\partial s} \cdot \frac{\partial \mathbf{r}}{\partial s} - 1\right) = \frac{1}{2}\left[\left(\frac{\partial x}{\partial s}\right)^2 + \left(\frac{\partial y}{\partial s}\right)^2 + \left(\frac{\partial z}{\partial s}\right)^2 - 1\right]. \tag{2.3}$$

Considering a cable element ds moving in a steady state and applying Newton's law to this body [13–17], we get:

$$\mathbf{M}\frac{d^2\mathbf{r}(s,t)}{dt^2} = \frac{d\mathbf{T}}{ds} + \sum \mathbf{F}. \tag{2.4}$$

In the above equation, $\mathbf{T}$ is the tension at the right end of cable's element, $\mathbf{M}$ is the diagonal inertia matrix of the concentrated mass, $d^2\mathbf{r}(s,t)/dt^2$ is accelerate, and $\mathbf{F}$ is the total external force, both corresponding at the unit of cable length, including gravity, damping force, and aerodynamic drag forces.

Starting from the significant operator $\mathrm{d}/\mathrm{d}t = (\partial/\partial t) + (\dot{L}\partial/\partial t)$, the velocity and the acceleration of the point P of curvilinear coordinate s are

$$\frac{\mathrm{d}\mathbf{r}}{\mathrm{d}t} = \frac{\partial\mathbf{r}}{\partial t} + \frac{\partial\mathbf{r}}{\partial s}\dot{L}, \tag{2.5}$$

$$\frac{\mathrm{d}^2\mathbf{r}}{\mathrm{d}t^2} = \frac{\partial^2\mathbf{r}}{\partial t^2} + 2\frac{\partial^2\mathbf{r}}{\partial s\partial t}\dot{L} + \frac{\partial^2\mathbf{r}}{\partial s^2}\dot{L}^2 + \frac{\partial\mathbf{r}}{\partial s}\ddot{L}, \tag{2.6}$$

where $\dot{L} = \mathrm{d}s/\mathrm{d}t$ is the cable velocity, and $\ddot{L} = \mathrm{d}^2s/\mathrm{d}t^2$ is the cable accelerate when the cable moves slowly. For the purposes of simplicity, we assume $\dot{L}^2 \approx 0$ and $\ddot{L} \approx 0$ when the cable moves slowly. Then from (2.6) we get

$$\frac{\mathrm{d}^2\mathbf{r}}{\mathrm{d}t^2} = \frac{\partial^2\mathbf{r}}{\partial t^2} + 2\frac{\partial^2\mathbf{r}}{\partial s\partial t}\dot{L}. \tag{2.7}$$

The dynamical equations for the cable are derived from (2.4) and (2.7).

By neglecting inertial force, the bending moments, and torsional moments of the cable in steady movement, a governing (2.4) for the cable can be expressed as

$$\frac{\mathrm{d}\mathbf{T}}{\mathrm{d}S} + \mathbf{B} + \mathbf{D} = 0. \tag{2.8}$$

Note that, $\mathbf{T} = T\boldsymbol{\tau}$, $\mathrm{d}\mathbf{T}/\mathrm{d}S = (T\mathrm{d}\boldsymbol{\tau}/\mathrm{d}s + \boldsymbol{\tau}\mathrm{d}T/\mathrm{d}s)(1 + \varepsilon)^{-1}$ where $\boldsymbol{\tau}$ is the intensity of the vector tension T. Within a slow motion of the cable, in what follows the radial force $T\mathrm{d}\boldsymbol{\tau}/\mathrm{d}s$ can be considered as negligible. $\mathbf{B}$ is the net gravitational force per unit length, $\mathbf{D}$ is aerodynamic drag forces. Substituting the force [16, 17] in (2.8) and rearranging the terms, we get

$$-m_0 g\mathbf{k} + 0.5\rho_a\pi d_0 C_F\sqrt{1+\varepsilon}\,|\boldsymbol{\mu}_\tau|\boldsymbol{\mu}_\tau,$$

$$-0.5\rho_a d_0 C_\mathrm{d}\sqrt{1+\varepsilon}\,|\boldsymbol{\mu}-\boldsymbol{\mu}_\tau|(\boldsymbol{\mu}-\boldsymbol{\mu}_\tau) + \left(\frac{T\mathrm{d}\boldsymbol{\tau}}{\mathrm{d}s} + \frac{\boldsymbol{\tau}\mathrm{d}T}{\mathrm{d}s}\right) = 0, \tag{2.9}$$

where m_0 is the mass per unit unstressed cable length. d_0 is diameter of the unstressed cross-section. ρ_a is air density. $\boldsymbol{\mu} = \mathrm{d}\mathbf{r}/\mathrm{d}t - \mathbf{J}$, $\mathbf{J}$ is wind velocity. $\boldsymbol{\mu}_\tau$ is the tangential component of $\boldsymbol{\mu}$ in local cable coordinates. C_d is the cable drag coefficient to the wind. C_F is drag coefficient surface friction factor. $C_F = C_m C_\mathrm{d}/\pi$, when the cable cross section is circle, $C_m = 0.02 \sim 0.05$, and $C_\mathrm{d} = 1.2$ [18].

Given conditions, time-domain simulation of the cable dynamics is obtained by propagating (2.9) in time through the use of a suitable temporal integration algorithm. In this work, adaptive Runge-Kutta algorithm is used.

3. A Three-Dimensional Dynamic Model of Deployment/Retrieval Cable

3.1. A Lumped Mass Method for Cable Dynamic Model

The cable is discretized into a series of N elastic segments joined at nodes, which are numbered by i from 0 at the downstream end to N at the upper end. The cable length coordinates satisfy $0 = s_0 < s_1 < \cdots < s_i < \cdots < s_N = S$. The mass of each segment is lumped in equal amounts at each of its two boundary nodes, by analogy the external forces are also lumped in this way. These segments are required to be small enough, so that the forces acting on them are approximately uniform over their length.

Applying Newton's second law to the node i, we get the governing equation

$$\mathbf{M}_i \ddot{\mathbf{x}}_i = \mathbf{F} = \Delta \mathbf{T}_i + \mathbf{W}_i + \mathbf{D}_i, \tag{3.1}$$

where the mass matrix $\mathbf{M}_i = m_i \mathbf{I}$, $\mathbf{I}$ represents 3×3 unit square matrix, $m_i = (\rho l^u{}_{i-1,j} + \rho l^u{}_{i,j+1})/2$, ρ is the mass per unit cable length, and l^u is the unstressed cable length between units. The subscript i and $i+1$ denote the physical terms between node i and $i+1$. As a whole cable, it is $\mathbf{x} = [x_1 y_1 z_1 \cdots x_i y_i z_i \cdots x_{n-1} y_{n-1} z_{n-1}]^T$, where $\mathbf{x}_i = [x_{i-1} y_{i-1} z_{i-1} \cdots x_{i+1} y_{i+1} z_{i+1}]^T$, $\ddot{\mathbf{x}}$ is the acceleration of the node.

The tension $\Delta \mathbf{T}_i$ of the node i is:

$$\Delta \mathbf{T}_i = \mathbf{T}_{i,j+1} - \mathbf{T}_{i-1,j}, \tag{3.2}$$

$\mathbf{T}_{i,j+1} = A_0 E \varepsilon_{i,j+1} \boldsymbol{\tau}_{i,j+1}$, $\varepsilon_{i,j+1} = (l_{i,i+1} - l^u{}_{i,i+1})/l^u{}_{i,i+1}$, where A_0 is the area of unstressed cross section, and $l_{i,i+1} = |r_{i+1} - r_i|$ is the length between node i and $i+1$. It can be expressed in recursive form as [19]. Different methods lead to the same results.

$\mathbf{W}_i$ is the gravity of node [20] i:

$$\mathbf{W}_i = -m_i g \mathbf{k}, \tag{3.3}$$

$\mathbf{D}_i$ [16] is the wind force of node i:

$$\mathbf{D}_i = \frac{(\mathbf{D}_{i-1,i} + \mathbf{D}_{i,i+1})}{2}. \tag{3.4}$$

3.2. Boundary and Initial Conditions

v_d is the velocity of deployment/retrieval cable, and it can be controlled. When the cable is deployed, $v_d < 0$. When the cable is retrieved, $v_d > 0$. Refer to Figure 3. When the cable is deployed or retrieved, its length at any time t can be determined by

$$s_{id}(t) = s_0 - \int_0^t \frac{v_d}{1 + \varepsilon} d\tau, \tag{3.5}$$

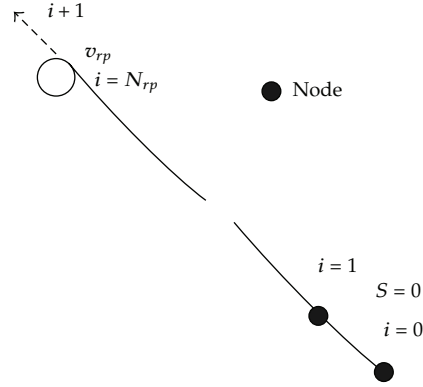where s_0 is the initial length of the cable at startup.

Figure 3: Discrete model of the cable deployment/retrieval.

3.3. Boundary Conditions of Cable Deployment/Retrieval

The cable force at the node 0, which is connected to the cabin, can be calculated in (3.1)

$$\mathbf{M}_0 \ddot{\mathbf{x}}_0 = \mathbf{F}_0 = \Delta \mathbf{T}_0 + \mathbf{W}_0 + \mathbf{D}_0 + \mathbf{f}_0, \tag{3.6}$$

where $\mathbf{M}_0 = (wl^u{}_{0,1}/2)\mathbf{I}$, $\Delta \mathbf{T}_0 = A_0 E \varepsilon_{0,1} \boldsymbol{\tau}_{0,1}$, $\mathbf{W}_0 = m_0 g \mathbf{k}$, $\mathbf{D}_0 = \mathbf{D}_{0,1}/2$, and $\mathbf{f}_0 = F_0$.

Refer to Figure 3. when the velocity of the node connected to pulley is v_{rp}, the cable length at any time t can be determined by

$$S = \begin{cases} s - \displaystyle\int_0^t \frac{v_{rp}}{1 + \varepsilon} \mathrm{d}t, & \text{retrieval,} \\[4mm] s + \displaystyle\int_0^t \frac{v_{rp}}{1 + \varepsilon} \mathrm{d}t, & \text{deployment,} \end{cases} \tag{3.7}$$

where the ε is the function of tension of node N and changes with time. Here we ignore the variations.

The position and velocity of the end node can be expressed as

$$x_N = x_{\text{pulley}},$$
$$\dot{x}_N = v_{rp} \tau_{rp}. \tag{3.8}$$

The subscript rp is the mark of deployment/retrieval. τ_{rp} is the tangent vector of the cable end node. $\tau_{N,N-1}$ is used to the numerical calculation.
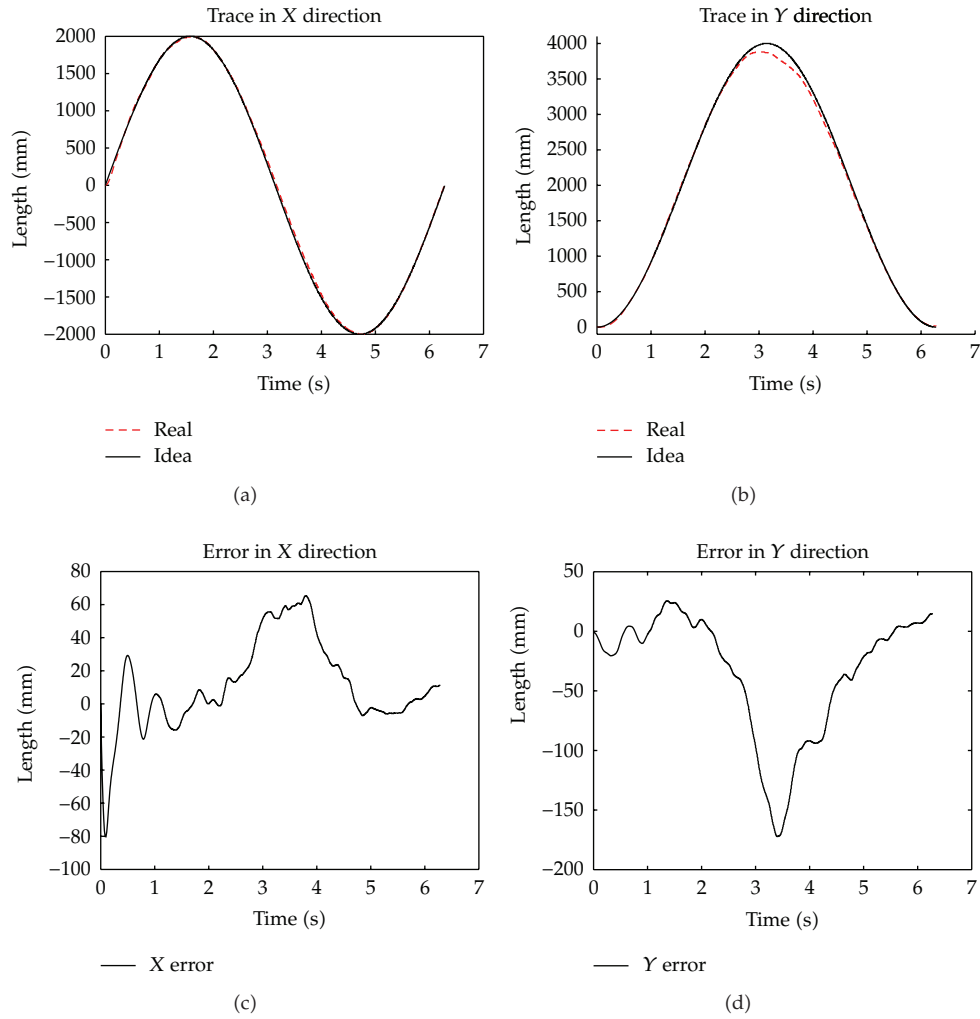
Figure 4: Trace and error of circle path.

The initial condition of the simulation is steady states of the cable movement. According to the governing equation, we get

$$\frac{\mathrm{d}\dot{x}_i}{\mathrm{d}t} = M_i^{-1}(\Delta\mathbf{T}_i + \mathbf{W}_i + \mathbf{D}_i)$$
$$(i = 1 \sim N - 1). \qquad (3.9)$$
$$\frac{\mathrm{d}x_i}{\mathrm{d}t} = \dot{x}_i$$

With the boundary condition and the initial condition, the nonlinear equations can be solved.
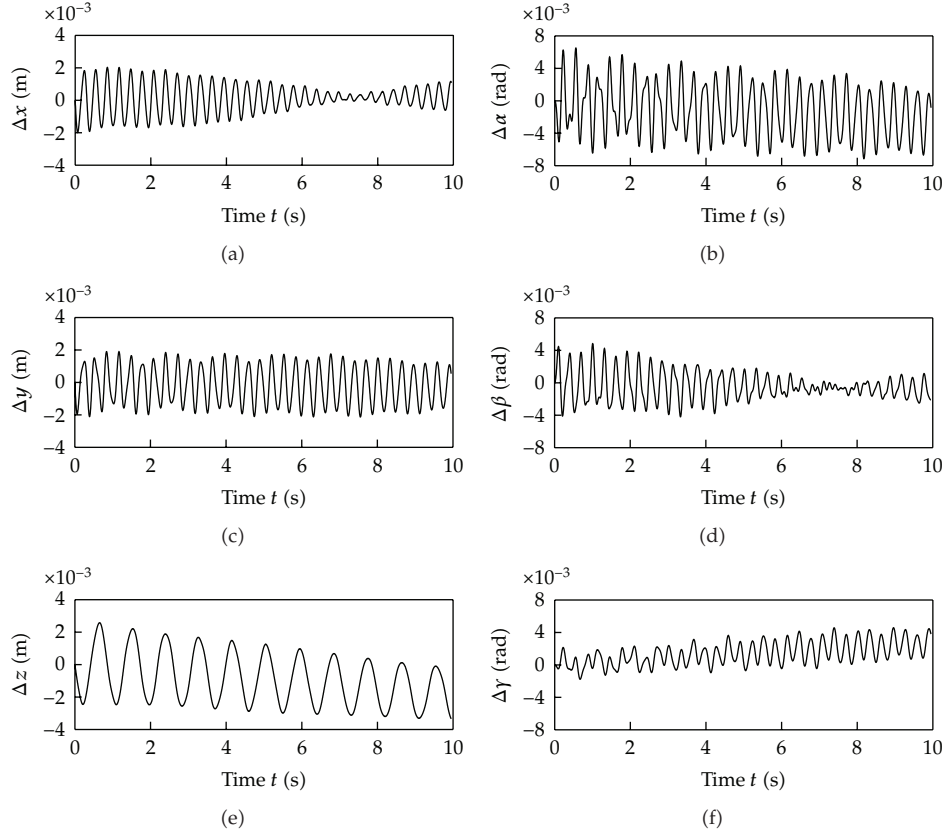
Figure 5: Error in line path.

4. Numerical Results of CDPR

(1) In the first simulation, the cabin tracks a moving target with constant velocity $v = 2\,\text{m/s}$ and constant pose ($\alpha = 0$, $\beta = 0$, γ is not limited). The initial point is $(0.0, 0.0, 9135.0, 0.0, 0.0, 0.0)^T$ (mm, rad). The geometric path is a circle with the radius of $2\,\text{m}$, parallel to the x-y plane. $(0, 1, -1470, 0, 0, 0)^T$ (mm, rad) is the error between current position and start position. Figure 4 shows the simulation result.

(2) In the second simulation, the cabin moves from the equilibrium position $(2.00, 1.00, 16.0, 0.0889, -0.1756, 3.108)^T$ (m, rad) to the end position $(2.50, 1.50, 16.2, 0.135, -0.263, 3.121)^T$ (mm, rad) in $10\,\text{s}$. The trace of each coordinate is line. There is no error between the equilibrium position and start position. Figure 5 shows the simulation result.

5. Conclusions

In this study, a computational dynamics model is developed to simulate the dynamics of variable length cable-driven parallel robot (CDPR) system. Numerical results show the effectiveness of the model to capture the complex cable dynamics where the cable length

is varying for it is gradually deployment or retrieval. When there is no error between current position and start position, the error values attenuate slowly, owing to little damp of cable system. When there is error between current position and start position, the dynamic characteristic of cable is significantly increased. We can find the changes of cabin position under impact loading, and the relevant researches and developing tendency [21] on the error between current position and start position versus trace errors will be researched.

List of Symbols

$\mathbf{i}, \mathbf{j}, \mathbf{k}$:	Three orthogonal unit vectors of the base frame XYZ
$\boldsymbol{\tau}, \mathbf{n}, \mathbf{b}$:	The unit vectors of the cable frame
s:	The length coordinate of the unstretched cable measured form its downstream end
$S(s, t)$:	The length of the stressed cable
$\mathbf{r}(s, t)$:	The position vector of a point on the continuous cable
$\mathbf{T}$:	The tension of at the right end of cable's element
$\mathbf{M}$:	The diagonal inertia matrix of the concentrated mass
$\mathrm{d}^2 \mathbf{r}(s, t) / \mathrm{d} t^2$:	Accelerate at the unit of cable length
$\mathbf{B}$:	Is the net gravitational force per unit length
$\mathbf{D}$:	Aerodynamic drag forces
m_0 :	The mass per unit unstressed cable length
d_0 :	Diameter of the unstressed cross section
ρ_a :	Air density
$\boldsymbol{\mu} = \mathrm{d}\mathbf{r}/\mathrm{d}t - \mathbf{J}$:	$\mathbf{J}$ is wind velocity
$\boldsymbol{\mu}_{\boldsymbol{\tau}}$:	The tangential component of μ in local cable coordinates
C_{d} :	The cable drag coefficient to the wind
C_F :	The surface friction factor
ρ :	The mass per unit cable length
l^u :	The unstressed cable length between units
$\mathbf{x}, \dot{\mathbf{x}}, \ddot{\mathbf{x}}$:	Displacements, velocities and accelerations of the node
$\Delta \mathbf{T}_i$:	The tension of the node i
$\mathbf{W}_i$:	The gravity of node i
$\mathbf{D}_i$:	The wind force of node i
v_d :	The velocity of deployment/retrieval cable
s_0 :	The initial length of the cable at startup
v_{rp} :	The velocity of the node connected to pulley
ε :	Is the function of tension of node N
τ_{rp} :	Is the tangent vector of the cable end node
$\tau_{N,N-1}$:	Is used to the numerical calculation
$\mathbf{F}$:	The total external force, corresponding to the unit of cable length.

Acknowledgment

References

[1] B. Y. Duan, Y. Zhao, J. Wang, and G. Xu, "Study of the feed system for a large radio telescope from the viewpoint of mechanical and structural engineering," in *Proceedings of the 3rd Meeting of the Large Telescope Working Group and of a Workshop on Spherical Radio Telescopes*, pp. 85–102, Gui-Zhou, China, 1995.

[2] B. Y. Duan, "A new design project of the line feed structure for large spherical radio telescope and its nonlinear dynamic analysis," *Mechatronics*, vol. 9, no. 1, pp. 53–64, 1999.

[3] T. Higuchi, A. Ming, and J. Jiang-Yu, "Application of multi-dimensional wire cranes in construction," in *Proceedings of the 5th International Symposium on Robotics in Construction (ISRC '88)*, pp. 661–668, Tokyo, Japan, 1988.

[4] J. Albus, R. Bostelman, and N. Dagalakis, "NIST ROBOCRANE," *Journal of Robotic Systems*, vol. 10, no. 5, pp. 709–724, 1993.

[5] A. B. Alp and S. K. Agrawal, "Cable suspended robots: design, planning and control," in *Proceedings of the IEEE International Conference on Robotics and Automation*, pp. 4275–4280, Washington, DC, USA, May 2002.

[6] P. Bosscher, A. T. Riechel, and I. Ebert-Uphoff, "Wrench-feasible workspace generation for cable-driven robots," *IEEE Transactions on Robotics*, vol. 22, no. 5, pp. 890–902, 2006.

[7] W. Shiang, D. Cannon, and J. Gorman, "Dynamic analysis of the cable array robotic crane," in *Proceedings of the IEEE International Conference on Robotics and Automation (ICRA '99)*, pp. 2495–2500, Detroit, Mich, USA, May 1999.

[8] M. Yamamoto, N. Yanai, and A. Mohri, "Trajectory control of incompletely restrained parallel-wire-suspended mechanism based on inverse dynamics," *IEEE Transactions on Robotics*, vol. 20, no. 5, pp. 840–850, 2004.

[9] F. Leonhardt and J. Schlaich, "Structural design of roofs over the sports arenas for the 1972 Olympic Games: some problems of prestressed cable net structures," *The Structural Engineer*, vol. 50, no. 3, pp. 113–119, 1972.

[10] F. Wang, G.-L. Huang, and D.-H. Deng, "Dynamic response analysis of towed cable during deployment/retrieval," *Journal of Shanghai Jiaotong University (Science)*, vol. 13, no. 2, pp. 245–251, 2008.

[11] Y. I. Choo and M. J. Casarella, "A survey of analytical methods for dynamic simulation of cable-body systems," *Journal of Hydronautics*, vol. 7, no. 4, pp. 137–144, 1973.

[12] B. Zi, B. Y. Duan, J. L. Du, and H. Bao, "Dynamic modeling and active control of a cable-suspended parallel robot," *Mechatronics*, vol. 18, no. 1, pp. 1–12, 2008.

[13] F. Milinazzo, M. Wilkie, and S. A. Latchman, "An efficient algorithm for simulating the dynamics of towed cable systems," *Ocean Engineering*, vol. 14, no. 6, pp. 513–526, 1987.

[14] C. M. Ablow and S. Schechter, "Numerical simulation of undersea cable dynamics," *Ocean Engineering*, vol. 10, no. 6, pp. 443–457, 1983.

[15] S. Huang, "Dynamic analysis of three-dimensional marine cables," *Ocean Engineering*, vol. 21, no. 6, pp. 587–605, 1994.

[16] P. Williams, "Deployment/retrieval optimization for flexible tethered satellite systems," *Nonlinear Dynamics*, vol. 52, no. 1-2, pp. 159–179, 2008.

[17] K. K. Mankala and S. K. Agrawal, "Dynamic modeling of satellite tether systems using Newton's laws and Hamilton's principle," *Journal of Vibration and Acoustics*, vol. 130, no. 1, Article ID 014501, 6 pages, 2008.

[18] J. Q. Cheng, et al., "Computing the the character of a cable in a uniform Stream," *China's Shipbuilding*, no. 1, pp. 51–64, 1980.

[19] S. Staicu, X.-J. Liu, and J. Li, "Explicit dynamics equations of the constrained robotic systems," *Nonlinear Dynamics*, vol. 58, no. 1-2, pp. 217–235, 2009.

[20] N. Riehl, M. Gouttefarde, S. Krut, C. Baradat, and F. Pierrot, "Effects of non-negligible cable mass on the static behavior of large workspace cable-driven parallel mechanisms," in *Proceedings of the IEEE International Conference on Robotics and Automation (ICRA '09)*, pp. 2193–2198, Kobe, Japan, May 2009.

[21] Y.-G. Tang, S.-X. Zhang, H.-Y. Zhang, and R.-Y. Zhang, "Snap tension induced by slack-taut in a mooring system," *Journal of Vibration and Shock*, vol. 27, no. 4, pp. 70–72, 2008.